

# Crystal Structure and Metamagnetic Behavior of the Ferrimagnetic Chain Compound MnCu(opba)(H<sub>2</sub>O)<sub>2</sub>·DMSO (opba = *o*-Phenylenebis(oxamato) and DMSO = Dimethyl Sulfoxide)

Humberto O. Stumpf,<sup>†,1</sup> Yu Pei,<sup>†</sup> Lahcène Ouahab,<sup>‡</sup> Françoise Le Berre,<sup>‡</sup> Epiphane Codjovi,<sup>†</sup> and Olivier Kahn<sup>\*,†</sup>

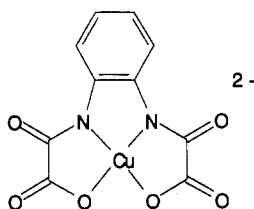
Laboratoire de Chimie Inorganique, URA No. 420, Université de Paris Sud, 91405 Orsay, France, and Laboratoire de Chimie du Solide et Inorganique Moléculaire, URA No. 1495, Université de Rennes 1, 35042 Rennes, France

Received June 9, 1993<sup>⊙</sup>

The title compound has been synthesized, and its crystal structure has been solved. It crystallizes in the triclinic system, space group  $P\bar{1}$ ; the lattice parameters are  $a = 7.300(3)$  Å,  $b = 10.734(3)$  Å,  $c = 12.585(6)$  Å,  $\alpha = 68.43(3)^\circ$ ,  $\beta = 84.92(4)^\circ$ ,  $\gamma = 73.97(3)^\circ$ , and  $Z = 2$ . The structure consists of oxamato-bridged Mn<sup>II</sup>Cu<sup>II</sup> chains running along the  $b$  axis with a Mn- -Cu intrachain separation of 5.387(1) Å. The chains pack above each other along the  $a$  axis with Mn- -Mn = 5.030(1) Å as the shortest metal- -metal interchain separation, forming bimetallic layers. These are separated by noncoordinated DMSO molecules along the  $c$  axis. The Mn(II) ion is in distorted octahedral environment, with two water molecules in *trans* positions; the Cu(II) ion is in planar environment. The magnetic susceptibility and the magnetization of the compound have been investigated. The  $\chi_M T$  versus  $T$  plot shows the minimum at 130 K characteristic of the one-dimensional ferrimagnetism, and a maximum at 8 K, related to a three-dimensional antiferromagnetic ordering at  $T_N = 5$  K. The intrachain interaction parameter has been found as  $J_{\text{MnCu}} = -32.1 \text{ cm}^{-1}$  ( $H = -J_{\text{MnCu}} \sum_i S_{\text{Mn},i} S_{\text{Cu},i}$ ). The field dependence of the magnetization has revealed a field-induced transition from an antiferromagnetic to a ferromagnetic-like state. A magnetic field of 5 kOe is sufficient to overcome the weak interchain antiferromagnetic interactions, so that the compound may be described as a metamagnet built from ferrimagnetic chains.

## Introduction

Recently we reported on a novel Mn<sup>II</sup>Cu<sup>II</sup> bimetallic chain compound resulting from the reaction of the Mn<sup>II</sup> ion with the Cu(II) precursor [Cu(opba)]<sup>2-</sup>



where opba stands for orthophenylenebis(oxamato). This compound, of formula MnCu(opba)(DMSO)<sub>3</sub>, has quite an unexpected zigzag chain structure, which is recalled in Figure 1. In contrast with the other Mn<sup>II</sup>Cu<sup>II</sup> chain compounds previously described, two oxamido groups are bound to the manganese atom in a *cis* fashion with a dihedral angle between the planes of the oxamato groups equal to 109.9°. This manganese atom completes its octahedral environment with two DMSO molecules, also in *cis* positions.<sup>2</sup> This peculiar structure has been of the utmost importance for us. Indeed, it suggested that it should be possible to replace the two DMSO molecules in the manganese coordination sphere by a third Cu(opba) group, and so to cross-link the chains and increase the dimensionality of the system. We succeeded in designing compounds of this kind with the stoichiometry C<sub>2</sub>Mn<sub>2</sub>[Cu(opba)]<sub>3</sub>nL where C<sup>+</sup> is a cation like NBU<sub>4</sub><sup>+</sup>

and L is a solvent molecule.<sup>2,3</sup> These compounds behave as molecular-based magnets; they show a spontaneous magnetization below a critical temperature on the order of 20 K.

When the structure of MnCu(opba)(DMSO)<sub>3</sub> was solved, we were wondering what were the factors governing the *cis* coordination around the manganese atom. It occurred to us that the apical DMSO molecule weakly bound to copper, owing to its bulkiness, could prevent the simultaneous presence of two neighboring manganese-bound DMSO molecules on the same side of the MnCu(opba) ribbon. To explore further this idea, we decided to replace the DMSO molecules by smaller ligands like H<sub>2</sub>O and to see whether the *cis* coordination was retained or not.

In this paper we report on a new compound in the Mn(II)/[Cu(opba)]<sup>2-</sup> system. Its formula is MnCu(opba)(H<sub>2</sub>O)<sub>2</sub>·DMSO. We will successively describe its synthesis, crystal structure, and physical properties. We will see that this compound is a metamagnet with a critical field of ca. 5 kOe. This work confirms the large variety of magnetic behaviors which can be observed with molecular bimetallic compounds.<sup>4-12</sup>

<sup>†</sup> Université de Paris Sud.

<sup>‡</sup> Université de Rennes.

<sup>⊙</sup> Abstract published in *Advance ACS Abstracts*, November 1, 1993.

(1) Permanent address: Departamento de Química, Universidade Federal de Minas Gerais, CEP 31270 Belo Horizonte, MG, Brazil.

- (2) Stumpf, H. O.; Pei, Y.; Kahn, O.; Sletten, J.; Renard, J. P. *J. Am. Chem. Soc.* **1993**, *115*, 6738.
- (3) Stumpf, H. O.; Ouahab, L.; Pei, Y.; Grandjean, D.; Kahn, O. *Science* **1993**, *261*, 447.
- (4) Kahn, O. *Struct. Bonding (Berlin)* **1987**, *68*, 89.
- (5) Kahn, O.; Pei, Y.; Journaux, Y. In *Inorganic Materials*, Bruce, D. W.; O'Hare, D., Eds.; John Wiley: Chichester, England, **1992**; p 59.
- (6) Sapina, F.; Coronado, E.; Beltran, D.; Burriel, R. *J. Am. Chem. Soc.* **1991**, *113*, 7940.
- (7) Gadet, V.; Mallah, T.; Castro, I.; Verdaguier, M. *J. Am. Chem. Soc.* **1992**, *114*, 9213.
- (8) Tamaki, H.; Zhong, Z. J.; Matsumoto, N.; Kida, S.; Koikawa, M.; Achiva, N.; Hashimoto, Y.; Okawa, H. *J. Am. Chem. Soc.* **1992**, *114*, 6974.
- (9) Sapina, F.; Escrivá, E.; Folgado, J. V.; Beltran, A.; Burriel, R.; Fuentetaja, A.; Drillon, M. *Inorg. Chem.* **1992**, *31*, 3851.
- (10) Lloret, F.; Ruiz, R.; Julve, M.; Faus, J.; Journaux, Y.; Castro, I.; Verdaguier, M. *Chem. Mater.* **1992**, *4*, 1150.
- (11) Guillou, O.; Kahn, O.; Oushoorn, R. L.; Boubekeur, K.; Batail, P. *Inorg. Chim. Acta* **1992**, *198-200*, 119.

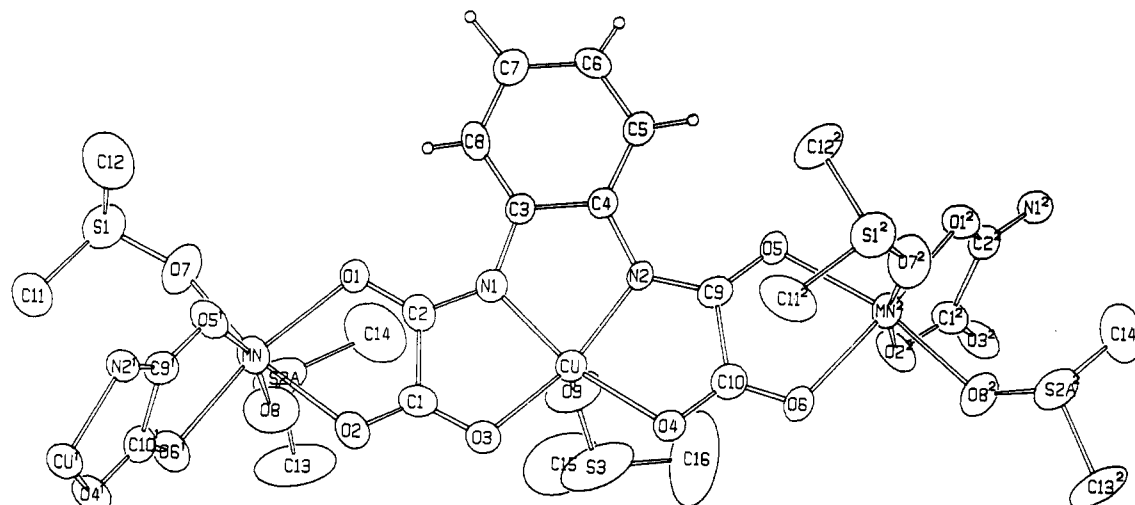


Figure 1. Recall of the zigzag chain structure of  $\text{MnCu}(\text{opba})(\text{DMSO})_3$  (from ref 2).

Table I. Crystallographic Data for  $\text{MnCu}(\text{opba})(\text{H}_2\text{O})_2\cdot\text{DMSO}$

chem formula: $\text{C}_{12}\text{H}_{14}\text{N}_2\text{O}_9\text{SCuMn}$	fw = 480.80
$a = 7.300(7) \text{ \AA}$	space group: $P\bar{1}$ (No. 2)
$b = 10.734(3) \text{ \AA}$	$T = 25 \text{ }^\circ\text{C}$
$c = 12.585(6) \text{ \AA}$	$\lambda = 0.710 73 \text{ \AA}$
$\alpha = 68.43(3)^\circ$	$\rho_{\text{calcd}} = 1.812 \text{ g cm}^{-3}$
$\beta = 84.92(4)^\circ$	$\mu = 20.587 \text{ cm}^{-1}$
$\gamma = 73.97(3)^\circ$	$r^a = 0.048$
$V = 881.4 \text{ \AA}^3$	$R_w^b = 0.062$
$Z = 2$	

<sup>a</sup>  $R = \sum(|F_o| - |F_c|) / \sum |F_o|$ . <sup>b</sup>  $R_w = [\sum w(|F_o| - |F_c|)^2 / \sum w(F_o)^2]^{1/2}$  with  $w = 4F_o^2 / [\sigma^2(F_o^2) + (0.07F_o^2)^2]$ .

### Experimental Section

**Synthesis.** The copper(II) precursor,  $\text{Na}_2[\text{Cu}(\text{opba})]\cdot 3\text{H}_2\text{O}$ , was prepared as already described.<sup>2</sup>  $\text{MnCu}(\text{opba})(\text{H}_2\text{O})_2\cdot\text{DMSO}$  was synthesized as follows:  $1.2 \times 10^{-3}$  mol (0.294 g) of  $\text{Mn}(\text{CH}_3\text{CO}_2)_4\cdot 4\text{H}_2\text{O}$  was added to a solution of  $10^{-3}$  mol (0.412 g) of  $\text{Na}_2[\text{Cu}(\text{opba})]\cdot 3\text{H}_2\text{O}$  dissolved in 80 mL of a DMSO/ $\text{H}_2\text{O}$  (45/55) mixture at 60  $^\circ\text{C}$ . The resulting mixture was stirred until it became limpid and then was allowed to stand at room temperature. Violet single crystals appeared within a few hours; they were filtered off, washed with the DMSO/ $\text{H}_2\text{O}$  mixture, and air-dried. Yield: 0.337 g (70% with respect to the copper(II) precursor). Anal. Calcd for  $\text{C}_{12}\text{H}_{14}\text{N}_2\text{O}_9\text{SCuMn}$ : C, 29.98; H, 2.91; N, 5.83; S, 6.67; Cu, 13.22; Mn, 11.43. Found: C, 29.72; H, 2.97; N, 5.63; S, 7.01; Cu, 13.23; Mn, 10.91.

**X-ray Data Collection and Structure Determination.** A crystal of dimensions  $0.2 \times 0.2 \times 0.12$  mm was mounted on an Enraf Nonius CAD4 diffractometer using graphite-monochromated Mo  $K\alpha$  radiation ( $\lambda = 0.710 73 \text{ \AA}$ ). The cell dimensions were refined by least-squares method from setting angles of 25 centered reflections with  $10 \leq 2\theta \leq 20^\circ$ . The crystal data are summarized in Table I; a full-length table of crystallographic data is given in the supplementary material. The intensities were collected by  $\theta$ - $2\theta$  scans. Three standard reflections were measured every hour and revealed no decay in intensities. One set of reflections was collected up to  $2\theta = 50^\circ$ . The Lorentz and polarization corrections were applied. The structure was solved by direct methods and successive Fourier difference syntheses, and was refined by weighted anisotropic full-matrix least-squares methods. The DMSO molecules are randomly distributed on two positions. After refinement of positional and anisotropic thermal parameters for all nonhydrogen atoms, the positions of the hydrogen atoms were calculated with  $d(\text{C}-\text{H}) = 1 \text{ \AA}$  and  $B_{\text{eq}} = 4 \text{ \AA}^2$ , and included as a fixed contributor to  $F_c$ . Scattering factors and corrections for anomalous dispersion were taken from ref 13. All calculations were performed on a microVax 3100 computer using the Enraf-Nonius Molen

Table II. Atomic Coordinates and Equivalent Isotropic Thermal Parameters

atom	x	y	z	$B, \text{ \AA}^2$
Cu	0.2525(1)	-0.08119(7)	0.18747(6)	2.86(2)
Mn	0.2535(1)	0.43567(8)	0.14792(8)	2.52(2)
O1	0.2534(7)	0.0204(4)	0.2880(3)	3.5(1)
O2	0.2638(7)	0.2303(4)	0.2728(3)	3.0(1)
O3	0.2734(6)	0.3107(4)	0.0403(3)	2.6(1)
O4	0.2538(7)	-0.2695(4)	0.2878(3)	3.3(1)
O5	0.2467(7)	-0.4670(4)	0.2724(4)	3.1(1)
O6	0.2308(6)	-0.3447(3)	0.0396(3)	2.49(9)
O1W	0.5546(7)	0.3990(5)	0.1386(4)	3.9(1)
O2W	-0.0505(7)	0.4813(5)	0.1374(4)	3.7(1)
N1	0.2631(7)	0.0871(4)	0.0667(4)	2.2(1)
N2	0.2375(7)	-0.1429(4)	0.0658(4)	2.4(1)
C1	0.2625(9)	0.1429(6)	0.2307(5)	2.7(1)
C2	0.2667(9)	0.1883(5)	0.0989(5)	2.2(1)
C3	0.2461(9)	-0.3428(5)	0.2309(5)	2.6(1)
C4	0.2374(9)	-0.2728(5)	0.0985(5)	2.3(1)
C5	0.2594(8)	0.0843(5)	-0.0436(5)	2.1(1)
C6	0.276(1)	0.1883(6)	-0.1460(5)	2.7(1)
C7	0.265(1)	0.1690(7)	-0.2466(6)	3.7(2)
C8	0.238(1)	0.0478(6)	-0.2488(5)	3.6(2)
C9	0.226(1)	-0.0598(6)	-0.1468(5)	3.0(2)
C10	0.2394(9)	-0.0446(5)	-0.0438(5)	2.2(1)
S1	0.7183(7)	0.3987(6)	0.4261(4)	7.0(1)
S1P	0.804(1)	0.227(1)	0.4208(5)	12.2(3)
O7S	0.714(2)	0.464(1)	0.2980(9)	7.9(4)
O8S	0.804(2)	0.270(1)	0.299(1)	6.6(4)
C11S	0.585(2)	0.262(2)	0.466(1)	13.1(6)
C12S	0.944(2)	0.311(3)	0.464(1)	25(1)

programs.<sup>14</sup> Atomic coordinates for the nonhydrogen atoms are given in Table II, and bond lengths and angles are given in Table III. The atom-labeling scheme is shown in Figure 2. Atomic coordinates for hydrogen atoms, and anisotropic thermal parameters are given in Supplementary Material.

**Magnetic Measurements.** These were carried out with two instruments, namely a Faraday-type magnetometer working in the 4-300 K temperature range and a SQUID magnetometer working down to 1.7 K with magnetic fields up to 80 kOe.

**EPR Spectra.** The X-band powder EPR spectra were recorded at various temperatures between 4.2 and 300 K with a ER 200D Bruker spectrometer equipped with a helium continuous-flow cryostat, a Hall probe, and a frequency meter.

### Description of the Structure

The structure consists of  $\text{Mn}^{\text{II}}\text{Cu}^{\text{II}}$  infinite chains running along the  $b$  axis. Adjacent Mn(II) and Cu(II) ions are bridged by an oxamate group, with a Mn - -Cu separation of 5.387(1)  $\text{ \AA}$ . The

(12) Lloret, F.; Julve, M.; Ruiz, R.; Journaux, Y.; Nakatani, K.; Kahn, O.; Sletten, J. *Inorg. Chem.* 1993, 32, 27.

(13) *International Table for X-ray Crystallography*; Kynoch Press, Birmingham, England; (present distributor: D. Reidel, Dordrecht, The Netherlands), 1974; Vol. IV.

(14) *Molen (Molecular Structure Enraf-Nonius)*; Enraf-Nonius: Delft, The Netherlands, 1990.

Table III. Bond Distances (Å) and Bond Angles (deg)

Cu-O1	1.952(5)	N1-C5	1.403(8)
Cu-O4	1.948(4)	N2-C4	1.301(7)
Cu-N1	1.902(4)	N2-C10	1.396(6)
Cu-N2	1.900(6)	C1-C2	1.547(8)
Mn-O2	2.172(3)	C3-C4	1.554(8)
Mn-O3	2.202(5)	C5-C6	1.382(7)
Mn-O5	2.171(5)	C5-C10	1.431(9)
Mn-O6	2.215(3)	C6-C7	1.37(1)
Mn-O1W	2.124(5)	C7-C8	1.38(1)
Mn-O2W	2.141(5)	C8-C9	1.391(8)
O1-C1	1.264(7)	C9-C10	1.38(1)
O2-C1	1.238(9)	S1-O7S	1.50(1)
O3-C2	1.261(6)	S1-C11S	1.87(2)
O4-C3	1.257(9)	S1-C12S	1.66(2)
O5-C3	1.238(7)	S1P-O8S	1.43(1)
O6-C4	1.263(9)	S1P-C11S	1.64(2)
N1-C2	1.298(9)	S1P-C12S	1.76(3)
O1-Cu-O4	105.9(2)	Cu-N1-C5	115.0(4)
O1-Cu-N1	85.1(2)	C2-N1-C5	129.9(4)
O1-Cu-N2	168.1(1)	Cu-N2-C4	114.3(4)
O4-Cu-N1	168.7(2)	Cu-N2-C10	115.2(4)
O4-Cu-N2	85.7(2)	C4-N2-C10	130.4(6)
N1-Cu-N2	83.5(2)	O1-C1-O2	124.4(6)
O2-Mn-O3	77.3(2)	O1-C1-C2	117.9(6)
O2-Mn-O5	95.5(2)	O2-C1-C2	117.7(5)
O2-Mn-O6	172.3(2)	O3-C2-N1	130.1(6)
O2-Mn-O1W	94.0(2)	O3-C2-C1	118.9(6)
O2-Mn-O2W	90.2(2)	N1-C2-C1	111.1(5)
O3-Mn-O5	172.5(1)	O7S-S1-C11S	107.3(8)
O3-Mn-O6	110.2(1)	O7S-S1-C12S	106.4(7)
O3-Mn-O1W	88.0(2)	C11S-S1-C12S	105(1)
O3-Mn-O2W	88.5(2)	O4-C3-O5	124.9(5)
O5-Mn-O6	77.1(1)	O4-C3-C4	117.5(5)
O5-Mn-O1W	90.4(2)	O5-C3-C4	117.6(6)
O5-Mn-O2W	93.8(2)	O6-C4-N2	129.8(5)
O6-Mn-O1W	88.2(2)	O6-C4-C3	118.7(5)
O6-Mn-O2W	88.3(2)	N2-C4-C3	111.6(6)
O1W-Mn-O2W	173.8(2)	N1-C5-C6	127.3(6)
N2-C10-C5	113.2(6)	N1-C5-C10	113.0(4)
N2-C10-C9	127.6(6)	C6-C5-C10	119.7(6)
C5-C10-C9	119.2(5)	C5-C6-C7	119.6(6)
Cu-O1-C1	110.8(4)	C6-C7-C8	121.6(6)
Mn-O2-C1	114.2(3)	C7-C8-C9	119.8(7)
Mn-O3-C2	111.7(4)	C8-C9-C10	120.0(7)
Cu-O4-C3	111.0(3)	O8S-S1P-C11S	109.9(8)
Mn-O5-C3	114.7(4)	O8S-S1P-C12S	109(1)
Mn-O6-C4	111.7(3)	C11S-S1P-C12S	111(1)
Cu-N1-C2	115.1(4)		

Mn(II) ion is in a distorted octahedral environment with four oxygen atoms coming from two oxamate groups in the equatorial plane and two water molecules in the apical positions. In contrast with MnCu(opba)(DMSO)<sub>3</sub>, the coordination around the manganese atom is *trans*. The Cu(II) ion is in a planar environment with two nitrogen and two oxygen atoms in the equatorial plane. MnCu(opba)(H<sub>2</sub>O)<sub>2</sub>·DMSO is the first structurally characterized Mn<sup>II</sup>Cu<sup>II</sup> chain in which the Cu(II) ion is not in square pyramidal surroundings. All the phenyl groups of the oxamate ligands are on the same side of the chain axis, while in MnCu(pba)-(H<sub>2</sub>O)<sub>3</sub>·2H<sub>2</sub>O and MnCu(pbaOH)(H<sub>2</sub>O)<sub>3</sub> the propylene groups were alternately on each side of the chain axis.<sup>15,16</sup>

The oxamate-bridged chains stack along the *a* axis in a zig-zag fashion to form sorts of layers as shown in Figures 2 and 3. The separation between two adjacent chains along *a* is equal to 3.48 Å. The shortest metal-metal interchain separations occur between such adjacent chains. They involve ions of the same nature: Mn-Mn(-*x*, -*y*, *z*) = 5.030(1) Å, Mn-Mn(1 - *x*, 1 - *y*, -*z*) = 5.032(1) Å, Cu-Cu(-*x*, -*y*, -*z*) = 5.690(1) Å, and Cu-Cu(1 - *x*, -*y*, -*z*) = 5.725(1) Å. The existence of two different Mn-Mn and Cu-Cu distances is due to the fact

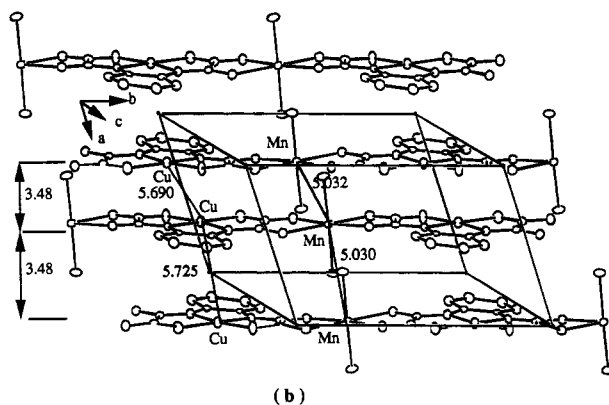
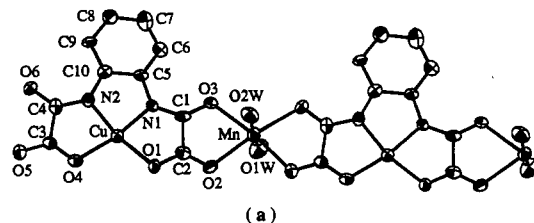


Figure 2. (a) Perspective view of a chain in MnCu(opba)(H<sub>2</sub>O)<sub>2</sub>·DMSO. (b) Projection of the structure down the *c* axis showing a layer (or a chain of chains) parallel to the *ab* plane.

that the chains along the *a* direction are related through an inversion center. The *ab* layers are separated along the *c* direction by the disordered DMSO molecules also forming layers as shown in Figure 3. The shortest metal-metal interchain separation along the *c* direction is Mn-Cu = 8.474 Å.

The chains are connected through hydrogen bonding: O1W-O6(1 - *x*, -*y*, -*z*) = 2.767(6) Å; O2W-O3(-*x*, 1 - *y*, -*z*) = 2.757(5) Å. Hydrogen bonding is also observed between bimetallic layers and DMSO molecules: O1W-O7S = 2.78(1) Å, O1W-O8S = 2.55(1) Å, O2W-O7S(*x* - 1, *y*, *z*) = 2.52(1) Å, O2W-O8S(*x* - 1, *y*, *z*) = 2.82(1) Å.

### Magnetic Properties

We will study the temperature dependence of the magnetic susceptibility, then the field and temperature dependences of the magnetization. Finally, we will describe the EPR spectra.

The magnetic susceptibility data are shown in Figure 4 in the form of the  $\chi_M T$  versus *T* plot,  $\chi_M$  being the molar magnetic susceptibility and *T* the temperature. The data below 20 K were measured with an applied field of 50 Oe, i.e. much lower than the critical field (*vide infra*). At room temperature  $\chi_M T$  is equal to 4.15 cm<sup>3</sup> K mol<sup>-1</sup>, which is slightly below what would be anticipated for uncoupled Mn(II) and Cu(II) ions. As the temperature is lowered,  $\chi_M T$  smoothly decreases and then reaches a rounded minimum about 130 K with  $\chi_M T = 3.93$  cm<sup>3</sup> K mol<sup>-1</sup>. When *T* is lowered further below 130 K,  $\chi_M T$  increases, then reaches a maximum at 8 K with  $\chi_M T = 13.51$  cm<sup>3</sup> K mol<sup>-1</sup>, and finally decreases rapidly between 8 and 1.7 K. This behavior is quite typical of ferrimagnetic chain compounds with weak antiferromagnetic interchain interactions. The maximum of  $\chi_M T$  at 8 K is related to a maximum of  $\chi_M$  at 5 K (see Figure 6). It is due to a three-dimensional antiferromagnetic ordering with a Neel temperature *T<sub>N</sub>* = 5 K.

To interpret quantitatively the susceptibility data, we successively utilized two approaches. First we considered the one-dimensional model described elsewhere<sup>17</sup> in which the magnetic susceptibility is deduced from a spin Hamiltonian of the form:

$$H = -J_{\text{MnCu}} \sum_{i=1}^n S_{\text{Mn},i} (S_{\text{Cu},i} + S_{\text{Cu},i-1}) \quad (1)$$

The summation runs over the *n* MnCu units along the chain.

(15) Pei, Y.; Verdaguer, M.; Kahn, O.; Sletten, J.; Renard, J. P. *Inorg. Chem.* **1987**, *26*, 138.

(16) Kahn, O.; Pei, Y.; Verdaguer, M.; Renard, J. P.; Sletten, J. *J. Am. Chem. Soc.* **1988**, *110*, 782.

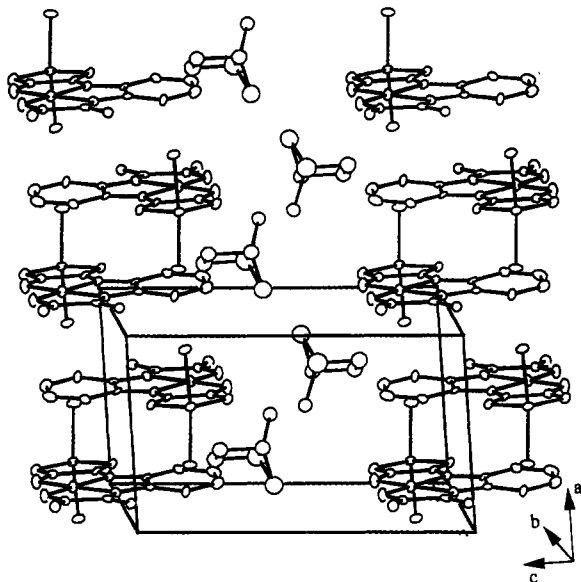


**Figure 3.** Perspective view of the structure of  $\text{MnCu}(\text{opba})(\text{H}_2\text{O})_2 \cdot \text{DMSO}$  down the  $b$  axis showing a layer of disordered DMSO molecules separating two bimetallic layers.

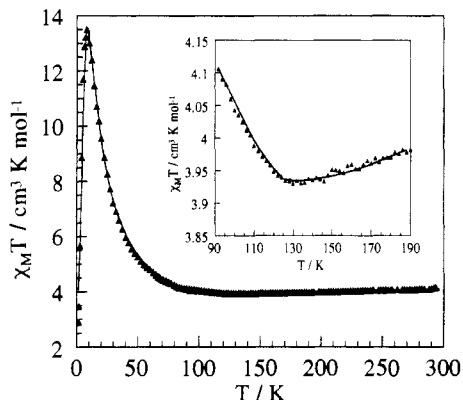


**Figure 4.** Experimental ( $\blacktriangle$ ) and calculated (—)  $\chi_M T$  versus  $T$  plot for  $\text{MnCu}(\text{opba})(\text{H}_2\text{O})_2 \cdot \text{DMSO}$ . The insert emphasizes the rounded minimum of  $\chi_M T$  around 130 K.

$J_{\text{MnCu}}$  is the interaction parameter between adjacent spin carriers.  $S_{\text{Mn}} = 5/2$  is treated as a classical spin and  $S_{\text{Cu}} = 1/2$  as a quantum spin. The parameters of this model in addition to  $J_{\text{MnCu}}$  are the local Zeeman factors  $g_{\text{Mn}}$  and  $g_{\text{Cu}}$ , assumed to be isotropic. This purely one-dimensional model is no longer valid in the low-temperature range where the interchain interactions perturb the magnetic data. Therefore, the fitting was limited to the 30–300 K range. The least-squares fitting of the experimental data with this model leads to  $J_{\text{MnCu}} = -32.1 \text{ cm}^{-1}$ ,  $g_{\text{Mn}} = 2.00$ , and  $g_{\text{Cu}} = 2.18$ . The agreement factor defined as  $\sum[(\chi_M T)^{\text{calc}} - (\chi_M T)^{\text{obs}}]^2 / [(\chi_M T)^{\text{obs}}]^2$  is then equal to  $3.5 \times 10^{-4}$  for 131 experimental points. As expected, the theoretical curve deduced from this one-dimensional approach passes above the experimental data below 30 K, since these experimental points are influenced by the antiferromagnetic interchain interactions.

The second approach consists of taking into account the interchain interactions in the paramagnetic phase, i.e. down to the onset of the three-dimensional antiferromagnetic ordering. In the preceding section, we pointed out that the structure of the compound, in addition to its dominant one-dimensional character, has some two-dimensional character. In the  $a$  direction the chains are much closer to each other than in the  $c$  direction, and form

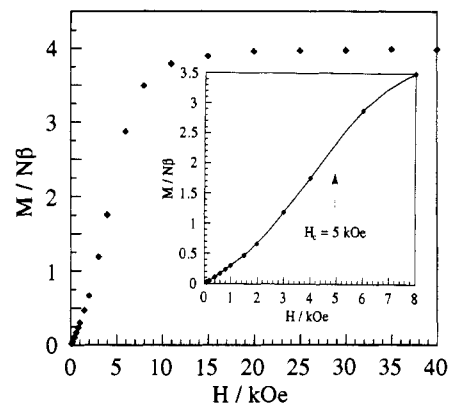


**Figure 5.** Magnetization  $M$  (in  $N\beta$  units) versus magnetic field plot at 1.7 K, i.e. below the Neel temperature. The insert emphasizes the change of sign of the second derivative  $\partial^2 M / \partial H^2$  around 5 kOe.

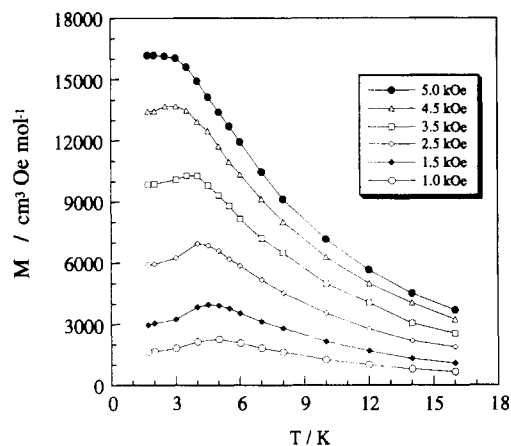


**Figure 6.**  $M$  versus  $T$  plots in the low-temperature range for various values of the applied magnetic field. The full lines joining the experimental points are just eye guides.

sorts of layers or chains of chains. At a given temperature  $T$ , the spin of a chain,  $S_{\text{chain}}$ , may be deduced from the theoretical  $\chi_M T$  value with the  $J_{\text{MnCu}}$ ,  $g_{\text{Mn}}$ , and  $g_{\text{Cu}}$  parameters given above, through

$$S_{\text{chain}}(S_{\text{chain}} + 1) = 3k(\chi_M T)^{\text{calc}} / Ng_{\text{chain}}^2 \beta^2 \quad (2)$$

where the Zeeman factor of a chain,  $g_{\text{chain}}$ , is taken as 2.00.  $S_{\text{chain}}$  is large enough to be treated as a classical spin. As a matter of fact,  $S_{\text{chain}}$  is calculated as 3.28 at 30 K, and 8.18 at 5 K. The interchain interactions along the  $a$  direction may then be described by the classical-spin approach according to<sup>18</sup>

$$\chi_M = \frac{Ng^2 \beta^2 S_{\text{chain}}(S_{\text{chain}} + 1)}{3kT} \frac{1+u}{1-u} \quad (3)$$

with

$$u = \coth[J'_a S_{\text{chain}}(S_{\text{chain}} + 1) / kT] - kT / S_{\text{chain}}(S_{\text{chain}} + 1) \quad (4)$$

$J'_a$  stands for the effective interchain interaction parameter along the  $a$  direction. Least-squares fitting of the experimental data down to the Neel temperature, 5 K, leads to  $J'_a = -0.05 \text{ cm}^{-1}$ . The agreement factor defined as above is then equal to  $9 \times 10^{-4}$  for 144 experimental points. The theoretical curve nicely describes the maximum of the  $\chi_M T$  versus  $T$  plot at 8 K (see Figure 4). The interchain interaction parameter along the  $c$  axis,  $J'_c$ , is anticipated to be much smaller than  $J'_a$ . Indeed, the interaction along  $c$  occurs through DMSO molecules with metal-metal

(17) Nakatani, K.; Carriat, J. Y.; Journaux, Y.; Kahn, O.; Lloret, F.; Renard, J. P.; Pei, Y.; Sletten, J.; Verdager, M. *J. Am. Chem. Soc.* **1989**, *111*, 5739.

(18) Fisher, M. E. *Am. J. Phys.* **1964**, *32*, 343.

separations larger than 8 Å. Approaches similar to that described above to estimate  $J'_a$  were already used.<sup>10,12,19</sup>

The variation of the magnetization  $M$  (in  $N\beta$  units) versus the applied magnetic field  $H$  at 1.7 K, i.e. below the Neel temperature, is shown in Figure 5. As the field is increased, the  $M$  versus  $H$  plot is linear up to ca. 2.5 kOe, then presents a signoidal variation with a change of sign for the second derivative  $\partial^2 M/\partial H^2$  around 5 kOe. Finally,  $M$  saturates with a saturation magnetization value of  $M_S = 4.0 N\beta$ , corresponding to what is expected for all the  $S_{Mn}$  local spins aligned along the field direction and all the  $S_{Cu}$  local spins aligned along the opposite direction. The change of sign for  $\partial^2 M/\partial H^2$  reveals a field-induced transition from an antiferromagnetic to a ferromagnetic-like state (we use the expression "ferromagnetic-like" because a genuine ferromagnetic state corresponds to a parallel spin alignment in zero field). A field of ca. 5 kOe is sufficient to overcome the weak antiferromagnetic interactions between the ferrimagnetic chains. MnCu(opba)(H<sub>2</sub>O)<sub>2</sub>·DMSO is a metamagnet.<sup>20</sup> This metamagnetic behavior is confirmed by the temperature dependences of the field-cooled magnetization at various fields shown in Figure 6. When  $H$  is below 5 kOe, the  $M$  versus  $T$  curve exhibits a maximum close to  $T_N = 5$  K. This maximum is less and less pronounced as  $H$  increases, and vanishes for  $H \geq 5$  kOe.

Metamagnetic behaviors in one-dimensional compounds were already observed for copper(II) ferromagnetic chains,<sup>21,22</sup> for ferrocenium charge-transfer salts forming ferromagnetic chains,<sup>23,24</sup> and recently for a ferromagnetic Mn<sup>III</sup>Cu<sup>II</sup> chain compound.<sup>10</sup>

The powder EPR spectrum for MnCu(opba)(H<sub>2</sub>O)<sub>2</sub>·DMSO exhibits a single and almost symmetrical band centered at  $g = 2.00$ , without detectable half-field transition. The line width at room temperature is 210 Oe and does not vary significantly versus temperature. This line width is slightly larger than for MnCu(opba)(DMSO)<sub>3</sub>, a compound in which the chains are almost perfectly isolated from each others.<sup>2</sup> This broadening might be due to the dipolar interactions along the  $c$  direction (see following section).

## Discussion and Conclusion

The first point we would like to discuss is the versatility of the crystal structures of the Mn<sup>II</sup>Cu<sup>II</sup> ferrimagnetic chains. In the same system Mn(II)/[Cu(opba)]<sup>2-</sup>, two chain compounds have been obtained to date. The former presents a *cis* coordination around the manganese atom resulting in a zigzag alternation of the metal ions; the latter compound shows the more usual *trans*

coordination around the manganese atom, resulting in a linear alternation of the metal ions. The factor governing the chain structure—zigzag or linear—seems to be the bulkiness of the apical ligands in both the manganese and copper coordination spheres. The copper atom in MnCu(opba)(H<sub>2</sub>O)<sub>2</sub>·DMSO has a planar environment without an apical ligand. Nothing prevents the ribbonlike structure with a *trans* coordination of the water molecules around the manganese atom.

The crystal structure of MnCu(opba)(H<sub>2</sub>O)<sub>2</sub>·DMSO has some other interesting peculiarities. First, in contrast with the other oxamato-bridged bimetallic chains,<sup>15,16</sup> the lateral groups of the bis(oxamato) ligands—the phenylene groups in the present case—are all on the same side of the chain axis. The site symmetry of the manganese atom, which was  $C_1$  in MnCu(pba)(H<sub>2</sub>O)<sub>3</sub>·2H<sub>2</sub>O<sup>15</sup> and close to  $C_1$  in MnCu(pbaOH)(H<sub>2</sub>O)<sub>3</sub>,<sup>16</sup> is close to  $C_{2v}$  in MnCu(opba)(H<sub>2</sub>O)<sub>2</sub>·DMSO; the 2-fold rotation axis lies in the equatorial plane, perpendicularly to the chain axis.

The association of the chains running along the  $b$  axis within the crystal lattice is also quite original. Along the  $a$  axis the chains pack above each other in a zigzag fashion, with short interchain separations, resulting in layers (or chains of chains). The compound has clearly some two-dimensional character. Along the third direction,  $c$ , the chains are separated by noncoordinated DMSO molecules, and the interchain distances are much longer. The structure as a whole may be described as consisting of an alternation of two kinds of layers, namely the Mn<sup>II</sup>Cu<sup>II</sup> chains of chains and the layers of DMSO molecules.

Let us now discuss briefly the magnetic properties. Down to ca. 30 K, the magnetic susceptibility data are governed by the one-dimensional ferrimagnetism. They are identical, within the experimental uncertainties, to those of the zigzag chain compound MnCu(opba)(DMSO)<sub>3</sub>, with the same value of the intrachain interaction parameter,  $J_{MnCu} = -32$  cm<sup>-1</sup>. This confirms the implicit assumption made to interpret the experimental data, namely that the interactions between next nearest neighbors are negligibly small.

The compound displays a three-dimensional antiferromagnetic ordering with a relatively high Neel temperature for this type of compounds,  $T_N = 5$  K. The antiferromagnetic nature of the interchain interactions along the  $a$  direction may be attributed to the fact that the shortest metal-metal separations along this direction involve metal ions of the same nature.<sup>16</sup> The interchain interactions along the  $c$  direction are most probably very weak, and rather of a dipolar nature. When an external field larger than 5 kOe is applied, the antiferromagnetic interchain interactions along the  $a$  direction are overcome, and all the  $S_{Mn}$  local spins are aligned in the direction of the field and the  $S_{Cu}$  local spins are aligned along the opposite direction. MnCu(opba)(H<sub>2</sub>O)<sub>2</sub>·DMSO is a metamagnet built from ferrimagnetic chains.

**Supplementary Material Available:** Tables SI–SIII, listing detailed crystallographic data, hydrogen atom coordinates, and anisotropic thermal parameters (3 pages). Ordering information is given on any current masthead page.

- (19) Caneschi, A.; Gatteschi, D.; Melandri, M. C.; Rey, P.; Sessoli, R. *Inorg. Chem.* **1990**, *29*, 4228.
- (20) Carlin, R. L. *Magnetochemistry*, Springer Verlag: New York, 1986.
- (21) Groenendijk, H. A.; van Duynevelt, A. J.; Blöte, H. W. J.; Gaura, R. M.; Willett, R. D. *Physica* **1980**, *106B*, 47.
- (22) Willett, R. D.; Landee, C. P.; Gaura, R. M.; Swank, D. D.; Groenendijk, H. A.; van Duynevelt, A. J. *J. Magn. Magn. Mater.* **1980**, *15–18*, 1055.
- (23) Candela, G. A.; Swartzendruber, L.; Miller, J. S.; Rice, M. J. *J. Am. Chem. Soc.* **1979**, *101*, 2755.
- (24) Broderick, W. E.; Thompson, J. A.; Hoffman, B. M. *Inorg. Chem.* **1991**, *30*, 2958.